Journal of Macromolecular Science, Part A
Publication details, including instructions for authors and subscription information:
http://www.informaworld.com/smpp/title~content=t713597274

Synthesis Of Side-Chain Liquid Crystalline Polymethacrylates Containing Fluorinated Diarylacetylene-Based Mesogenic Side Groups

Yann-Huei Wu[a]; Yong-Hong Lu[a]; Chain-Shu Hsu[a]
[a] Department of Applied Chemistry, National Chiao Tung University, Hsinchu, Taiwan, Republic of China

To cite this Article Wu, Yann-Huei , Lu, Yong-Hong and Hsu, Chain-Shu(1995) 'Synthesis Of Side-Chain Liquid Crystalline Polymethacrylates Containing Fluorinated Diarylacetylene-Based Mesogenic Side Groups', Journal of Macromolecular Science, Part A, 32: 8, 1471 — 1488

To link to this Article: DOI: 10.1080/10601329508013692

URL: http://dx.doi.org/10.1080/10601329508013692

J.M.S.—PURE APPL. CHEM., A32(8&9), pp. 1471–1488 (1995)

SYNTHESIS OF SIDE-CHAIN LIQUID CRYSTALLINE POLYMETHACRYLATES CONTAINING FLUORINATED DIARYLACETYLENE-BASED MESOGENIC SIDE GROUPS

YANN-HUEI WU, YONG-HONG LU, and CHAIN-SHU HSU*

Department of Applied Chemistry
National Chiao Tung University
Hsinchu, Taiwan 30050, Republic of China

ABSTRACT

The synthesis and characterization of side-chain liquid crystalline polymetnacrylates containing fluorinated diphenylacetylenic and naphthylphenylacetylenic side groups are presented. The phase behavior of the prepared monomers and polymers was characterized by differential scanning calorimetry, optical polarizing microscopy, and x-ray diffraction. All of the methacrylate monomers exhibit no mesomorphic behavior. Polymers which contain eleven methylene units in their spacers reveal smectic mesomorphism. Polymers with a short spacer length, i.e., three or six methylene units, present either a nematic phase or no mesophase. The glass transition temperatures of the obtained polymers decrease as the spacer length increases. The polymers containing fluorinated naphthylphenylacetylenic side groups show a higher tendency to form a mesophase than those containing fluorinated diphenylacetylenic side groups. Incorporation of a lateral fluoro-substituent in the mesogenic core decreases not only the possibility to form a mesophase but also the thermal stability of the mesophase.

INTRODUCTION

Side-chain liquid crystalline polymers (LCPs) are of both theoretical and practical interest because they combine the anisotropic properties of liquid crystals with polymeric properties and have the potential of being used for some new applications [1-10]. In recent years the synthesis of some new LCPs containing tolane- or diphenyldiacetylene-based mesogenic side groups has been presented [11-20]. These LC polymers, which have an extended π-conjugation and a perfect linear-rodlike mesogenic structure, exhibit extraordinarily high birefringence values and demonstrated potential for some new electro-optical devices [21, 22].

The goal of this study is to present the synthesis and characterization of side-chain LC polymethacrylates containing either fluorinated diphenylacetylene (tolane) or naphthylphenylacetylene side groups. The obtained polymers were characterized by differential scanning calorimetry, optical polarizing microscopy, and x-ray diffractometry. The thermal behavior of the prepared polymers is discussed.

EXPERIMENTAL

Materials

2-Methyl-3-butyn-2-ol, 1-fluoro-4-iodobenzene, and 1-bromo-3,4-difluorobenzene were obtained from Janssen Inc. and were used as received. Methacrylol chloride was also purchased from Janssen Inc. and was distilled before use. 4-Bromophenol and all other reagents were obtained from Aldrich, and they were used as received. Dichloromethane used in the esterification was refluxed over calcium hydride, and 1,4-dioxane was first refluxed over sodium; both were then distilled under nitrogen. 2,2′-Azobisisobutyronitrile (AIBN) (from Fluka Inc.) was freshly recrystallized from methanol.

Techniques

^{1}H-NMR spectra (300 MHz) were recorded on a Varian VXR-300 spectrometer. Thermal transitions and thermodynamic parameters were determined by using a Seiko SSC/5200 differential scanning calorimeter equipped with a liquid nitrogen cooling accessory. Heating and cooling rates were 10°C/min. The thermal transitions reported were collected during the second heating and cooling scans. A Carl-Ziess Axiphot optical polarized microscope equipped with a Mettler FP 82 hot stage and a FP 80 central processor was used to observe the thermal transitions and to analyze the anisotropic textures. Gel permeation chromatography (GPC) was run on an Applied Biosystems 400 LC instrument equipped with a differential refractometer, a UV detector, and a set of PL gel columns of 10^2, 5×10^2, 10^3, and 10^4 Å. The molecular weight calibration curve was obtained by using standard polystyrenes. X-ray diffraction measurements were performed with nickel-filtered CuKα radiation with a Rigaku powder diffractometer.

Synthesis of Monomers IM–XIIM

The synthesis of fluorinated diphenylacetylenic or naphthylphenylacetylenic monomers is outlined in Scheme 1.

1-Bromo-4-(3-hydroxypropan-1-yloxy)benzene (1)
1-Bromo-4-(6-hydroxyhexan-1-yloxy)benzene (2)
1-Bromo-4-(11-hydroxyundecan-1-yloxy)benzene (3)
2-Bromo-6-(3-hydroxypropan-1-yloxy)naphthalene (4)
2-Bromo-6-(6-hydroxyhexan-1-yloxy)naphthalene (5)
2-Bromo-6-(11-hydroxyundecan-1-yloxy)naphthalene (6)

All six compounds were prepared by etherification of 4-bromophenol or 2-bromo-6-naphthol with the corresponding 3-bromopropanol, 6-chlorohexanol, or 11-bromoundecanol. The synthesis of Compound **2** is described below.

4-Bromophenol (25 g, 0.144 mol) was added to a stirred solution of KOH (9.3 g, 0.166 mol) and KI (0.2 g) in 300 mL of 95% ethanol. 6-Chlorohexanol (2.7 g, 0.166 mol) was added when dissolution was complete. The solution was heated under reflux for 12 hours and cooled to room temperature. The solvent was then removed in a rotary evaporater. The residue was washed with water, dried, and purified by column chromatography (silica gel, ethyl acetate:*n*-hexane = 1:1 as eluent) to yield 33.2 g (84.5%) of a pale yellow liquid. ^{1}H NMR ($CDCl_3$, δ, ppm): 1.25–1.80 (m, 8H, $-(C\underline{H}_2)_4-CH_2-O-$), 3.62 (t, 2H, $HO-C\underline{H}_2-$), 3.96 (t, 2H, $-C\underline{H}_2-O-Ph-$), 6.83–7.44 (m, 4 aromatic protons).

2-Methyl-4-[4-(3-hydroxypropan-1-yloxy)phenyl]butyn-2-ol (7)
2-Methyl-4-[4-(6-hydroxyhexan-1-yloxy)phenyl]butyn-2-ol (8)
2-Methyl-4-[4-(11-hydroxyundecan-1-yloxy)phenyl]butyn-2-ol (9)
2-Methyl-4-[6-(3-hydroxypropan-1-yloxy)-2-naphthyl]butyn-2-ol (10)
2-Methyl-4-[6-(6-hydroxyhexan-1-yloxy)-2-naphthyl]butyn-2-ol (11)
2-Methyl-4-[6-(11-hydroxyundecan-1-yloxy)-2-naphthyl]butyn-2-ol (12)

All six compounds were prepared by the same method. The synthesis of Compound **8** is described below.

To a homogeneous solution of 1-bromo-4-(6-hydroxyhexan-1-yloxy)benzene (7 g, 0.026 mol) and 2-methyl-3-butyn-2-ol (2.39 g, 0.028 mol) in triethylamine (50 mL) was added bis(triphenylphosphine) palladium(II) chloride (70 mg), cuprous iodide (70 mg) and triphenyl phosphine (140 mg). The reaction mixture was heated under reflux for 8 hours, cooled to room temperature, and treated with saturated ammonium chloride solution. The obtained mixture was extracted with methylene chloride. The collected organic solution was washed with dilute hydrochloric acid and water and dried with anhydrous $MgSO_4$. After removal of the solvent, the remaining solid was purified by column chromatography (silica gel, ethyl acetate: *n*-hexane = 1:1 as eluent) to yield 4.5 g (63.5%) of 2-methyl-4-[4-(6-hydroxyhexan-1-yloxy)-phenyl]butyn-2-ol. ^{1}H NMR ($CDCl_3$, δ, ppm): 1.25–1.80 (m, 8H, $-(C\underline{H}_2)_4-CH_2-O-$), 1.60 (s, 6H, two $-C\underline{H}_3$), 3.62 (t, 2H, $HO-C\underline{H}_2-$), 3.96 (t, 2H, $-C\underline{H}_2-O-Ph-$), 6.83–7.44 (m, 4 aromatic protons).

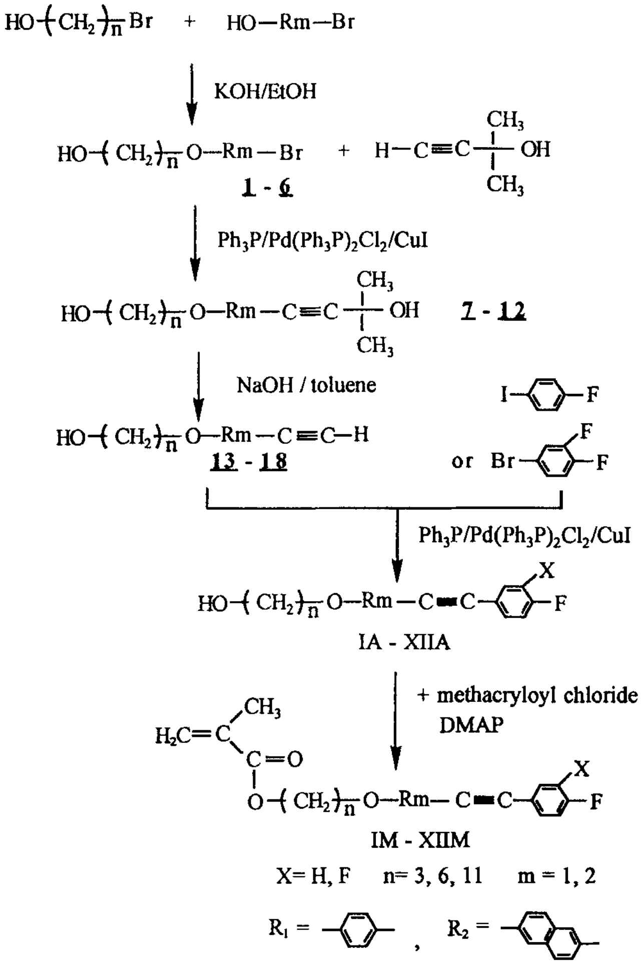

compound	IA	IIA	IIIA	IVA	VA	VIA	VIIA	VIIIA	IXA	XA	XIA	XIIA
monomer	IM	IIM	IIIM	IVM	VM	VIM	VIIM	VIIIM	IXM	XM	XIM	XIIM
Rm	R_1	R_1	R_1	R_1	R_1	R_1	R_2	R_2	R_2	R_2	R_2	R_2
n	3	6	11	3	6	11	3	6	11	3	6	11
X	H	H	H	F	F	F	H	H	H	F	F	F

SCHEME 1. Synthesis of methacrylate Monomers **IM–XIIM**.

4-(3-Hydroxypropan-1-yloxy)phenylacetylene (13)
4-(6-Hydroxyhexan-1-yloxy)phenylacetylene (14)
4-(11-Hydroxyundecan-1-yloxy)phenylacetylene (15)
6-(3-Hydroxypropan-1-yloxy)-2-naphthylacetylene (16)
6-(6-Hydroxyhexan-1-yloxy)-2-naphthylacetylene (17)
6-(11-Hydroxyundecan-1-yloxy)-2-naphthylacetylene (18)

All six compounds were prepared by the same method. The synthesis of Compound **14** is described below.

Compound **8** (3.0 g, 0.011 mol) was added to a solution of 0.88 g (0.022 mol) of sodium hydroxide in toluene (70 ml). The reaction mixture was heated under reflux for 4 hours, cooled, and filtered. After removal of the solvent, the crude product was purified by column chromatography (silica gel, ethyl acetate:*n*-hexane = 1:1 as eluent) to yield 1.45 g (60.5%) of white crystals; mp = 51.6°C. ^{1}H NMR ($CDCl_3$, δ, ppm): 1.25-1.80 (m, 8H, $-(C\underline{H}_2)_4-CH_2-O-$), 3.00 (s, 1H$-C{\equiv}C-\underline{H}$), 3.62 (t, 2H, $HO-C\underline{H}_2-$), 3.96 (t, 2H, $-C\underline{H}_2-O-Ph-$), 6.83-7.44 (m, 4 aromatic protons).

1-[4-(ω-Hydroxyalkan-1-yloxy)phenyl]-2-(4-fluorophenyl)acetylenes (IA–IIIA)
1-[4-(ω-Hydroxyalkan-1-yloxy)phenyl]-2-(3,4-difluorophenyl)acetylenes (IVA–VIA)
1-[6-(ω-Hydroxyalkan-1-yloxy)-2-naphthyl]-2-(4-fluorophenyl)acetylenes (VII–IXA)
1-[6-(ω-Hydroxyalkan-1-yloxy)-2-naphthyl]-2-(3,4-difluorophenyl)acetylenes (XA–XIIA)

Compounds **IA–XIIA** were prepared by the same method. The synthesis of Compound **VIA** is described below.

To a homogeneous solution of Compound **15** (2.50 g, 8.70 mmol) and 1-bromo-3,4-difluorobenzene (2.01 g, 10.42 mmol) in triethylamine (50 mL) was added bis(triphenylphosphine)palladium(II) chloride (35 mg), cuprous iodide (35 mg), and triphenyl-phosphine (70 mg). The reaction mixture was heated under reflux for 8 hours, cooled to room temperature, and treated with saturated ammonium chloride solution. The obtained mixture was extracted with methylene chloride. The collected organic solution was washed with dilute hydrochloric acid and water and dried with anhydrous $MgSO_4$. After removal of the solvent, the remaining solid was purified by column chromatography (silica gel, ethyl acetate:*n*-hexane = 1:4 as eluent) and finally recrystallized from *n*-hexane to yield 1.64 g (47.3%) of white crystals; mp = 74.8°C. ^{1}H NMR ($CDCl_3$, δ, ppm): 1.25-1.83 (m, 18H, $-(CH_2)_9-CH_2-O-$), 3.62 (t, 2H, $HO-C\underline{H}_2-$), 3.96 (t, 2H, $-CH_2-O-Ph-$), 6.82-7.60 (m, 7 aromatic protons).

Synthesis of Methacrylate Monomers IM–XIIM

All the methacrylate Monomers **IM–XIIM** were synthesized by the esterification of the corresponding Alcohols **IA–XIIA** with methacryloyl chloride. The preparation of Monomer **VIM** is described below.

Compound **VIA** (0,80 g, 2.0 mmol) was dissolved in a mixture of dried methylene chloride (50 mL) and 4-(dimethylamino)pyridine (DMAP, 0.29 g, 2.4 mmol). The resulting solution was cooled in an ice-water bath to 0°C, and methacryloyl chloride (0.63 g, 6.03 mmol) was added dropwise. The reaction mixture was allowed to warm slowly to room temperature and then stirred overnight. After the solution was poured into water, the precipitated product was filtered, dried under vacuum, purified by column chromatography (silica gel, ethyl acetate:*n*-hexane = 1:15 as eluent), and finally recrystallized from *n*-hexane to yield 0.35 g (37.4%) of white crystals. The yields and ^{1}H NMR chemical shifts of Monomers **IM–XIIM** are summarized in Table 1.

TABLE 1. Characterization of Methacrylate Monomers **IM–XIIM**

Monomer	R_m[a]	*n*[a]	X[a]	Yield, %	300 MHz ^{1}H NMR ($CDCl_3$, δ, ppm)
IM	R_1	3	H	48.2	1.95 (s, 3H, $-C\underline{H}_3$), 2.18 (m, 2H, $-C\underline{H}_2-CH_2-O-$), 4.11 (t, 2H, $-C\underline{H}_2-O-Ph$), 4.36 (t, 2H, $-COO-C\underline{H}_2-$), 5.58 and 6.11 (2s, 2H, $\underline{H}_2C=$), 6.80–7.60 (m, 8H, aromatic protons)
IIM	R_1	6	H	50.4	1.25–1.80 (m, 8H, $-(C\underline{H}_2)_4-CH_2-O-$), 1.95 (s, 3H, $-C\underline{H}_3$), 3.96 (t, 2H, $-C\underline{H}_2-O-Ph-$), 4.14 (t, 2H, $-COO-C\underline{H}_2-$), 5.58 and 6.11 (2s, 2H, $\underline{H}_2C=$), 6.80–7.60 (m, 8H, aromatic protons)
IIIM	R_1	11	H	41.6	1.25–1.83 (m, 18H, $-(C\underline{H}_2)_9-CH_2-O-$), 1.95 (s, 3H, $-C\underline{H}_3$), 3.96 (t, 2H, $-C\underline{H}_2-O-Ph-$), 4.14 (t, 2H, $-COO-C\underline{H}_2-$), 5.58 and 6.11 (2s, 2H, $\underline{H}_2C=$), 6.80–7.60 (m, 8H, aromatic protons)
IVM	R_1	3	F	37.8	1.95 (s, 3H, $-C\underline{H}_3$), 2.18 (m, 2H, $-C\underline{H}_2-CH_2-O-$), 4.11 (t, 2H, $-C\underline{H}_2$-O-Ph), 4.36 (t, 2H, $-COO-C\underline{H}_2-$), 5.58 and 6.11 (2s, 2H, $\underline{H}_2C=$), 6.80–7.60 (m, 7H, aromatic protons)
VM	R_1	6	F	42.6	1.25–1.80 (m, 8H, $-(C\underline{H}_2)_4-CH_2-O-$), 1.95 (s, 3H, $-C\underline{H}_3$), 3.96 (t, 2H, $-C\underline{H}_2-O-Ph-$), 4.14 (t, 2H, $-COO-C\underline{H}_2-$), 5.58 and 6.11 (2s, 2H, $H_2C=$), 6.80–7.60 (m, 7H, aromatic protons)
VIM	R_1	11	F	37.4	1.25–1.83 (m, 18H, $-(C\underline{H}_2)_9-CH_2-O-$), 1.95 (s, 3H, $-C\underline{H}_3$), 3.96 (t, 2H, $-C\underline{H}_2-O-Ph-$), 4.14 (t, 2H, $-COO-C\underline{H}_2-$), 5.58 and 6.11 (2s, 2H, $\underline{H}_2C=$), 6.80–7.60 (m, 7H, aromatic protons)
VIIM	R_2	3	H	42.9	1.96 (s, 3H, $-C\underline{H}_3$), 2.25 (m, 2H, $-C\underline{H}_2-CH_2-O-$), 4.20 (t, 2H, $-C\underline{H}_2-O-Ar-$), 4.40 (t, 2H, $-COO-C\underline{H}_2-$), 5.58 and 6.14 (2s, 2H, $\underline{H}_2C=$), 7.06–7.70 (m, 10H, aromatic protons)

VIIIM	R_2	6	H	40.7	1.38–1.86 (m, 8H, $-(C\underline{H}_2)_4-CH_2-O-O$, 1.88 (s, 3H, $-C\underline{H}_3$), 3.99 (t, 2H, $-C\underline{H}_2-O-Ar-$), 4.10 (t, 2H, $-COO-C\underline{H}_2-$), 5.47 and 6.03 (2s, 2H, $\underline{H}_2C=$), 6.98–7.89 (m, 10H, aromatic protons)
IXM	R_2	11	H	38.7	1.24–1.90 (m, 18H, $-(C\underline{H}_2)_9-CH_2-O-$), 1.94 (s, 3H, $-C\underline{H}_3$), 4.07 (t, 2H, $-C\underline{H}_2-O-Ar-$), 4.13 (t, 2H, $-COO-C\underline{H}_2-$), 5.54 and 6.10 (2s, 2H, $\underline{H}_2C=$), 7.05–7.96 (m, 10H, aromatic protons)
XM	R_2	3	F	87.6	1.95 (s, 3H, $-C\underline{H}_3$), 2.27 (m, 2H, $-C\underline{H}_2-CH_2-O-$), 4.23 (t, 2H, $-C\underline{H}_2-O-Ar-$), 4.46 (t, 2H, $-COO-C\underline{H}_2-$), 5.57 and 6.18 (2s, 2H, $\underline{H}_2C=$), 7.05–7.95 (m, 9H, aromatic protons)
XIM	R_2	6	F	41.1	1.42–1.88 (m, 8H, $-(C\underline{H}_2)_4-CH_2-O-$), 1.93 (s, 3H, $-C\underline{H}_3$), 4.01 (t, 2H, $-C\underline{H}_2-O-Ar-$), 4.12 (t, 2H, $-COO-C\underline{H}_2-$), 5.45 and 6.00 (2s, 2H, $\underline{H}_2C=$), 7.00–7.90 (m, 9H, aromatic protons)
XIIM	R_2	11	F	42.5	1.24–1.82 (m, 18H, $-(C\underline{H}_2)_9-CH_2-O-$), 1.87 (s, 3H, $-C\underline{H}_3$), 3.98 (t, 2H, $-C\underline{H}_2-O-Ar-$), 4.07 (t, 2H, $-COO-C\underline{H}_2-$), 5.46 and 6.12 (2s, 2H, $\underline{H}_2C=$), 7.00–7.89 (m, 9H, aromatic protons)

[a] According to Scheme 1.

Synthesis of Polymethacrylates IP–XIIP

The radical polymerizations of the monomers were carried out in Schlenk tubes equipped with septa under argon. The polymerization tube containing the 1,4-dioxane solution of the monomer (10%, w/v) and the initiator (AIBN, 1 wt% vs monomer) was first degassed by several freeze-pump-thaw cycles under vacuum and then filled with argon. All polymerizations were carried out at 60°C for 15 hours. After the polymerization time, the polymers were precipitated into methanol, filtered, and purified by reprecipitation from THF solutions into hot *n*-hexane. The polymerization results are summarized in Table 4.

RESULTS AND DISCUSSION

The synthetic routes used to prepare the Monomers **IM–XIIM** are outlined in Scheme 1. All the diphenylacetylenes or naphthylphenylacetylenes were prepared by coupling of terminal acetylene with 4-fluoroiodobenzene or 1-bromo-3,4-difluorobenzene. The terminal acetylenes were synthesized according to the procedures reported by Corey and Fuchs [23]. In addition to the cross-coupling products, a trace amount of homocoupling diaryldiacetylenic products was also formed. Therefore, the products should be purified several times by column chromatography and recrystallization. Table 1 summarizes the yields and ^{1}H NMR chemical shifts of the synthesized diphenylacetylenic and naphthylphenylacetylenic Monomers **IM–XIIM**.

The thermal transitions and the corresponding enthalpy changes of the fluorinated diphenylacetylenic and naphthylphenylacetylenic Compounds **IA–XIIA** are summarized in Table 2. Among Compounds **IA–VIA**, which contain a diphenylacetylene mesogenic core, Compound **VA** is the only one exhibiting monotropic nematic and smectic A phases. For Compounds **VIIA–XIIA**, a more bulky naphthyl ring has been used instead of a phenyl ring in the mesogenic core. All of the compounds except **VIIA** and **IXA** show mesomorphic behavior. Compounds **VIIIA**, **XA**, and **XIA** display a monotropic nematic phase, while Compound **XIIA** exhibits monotropic nematic and smectic A phases. Figure 1 presents the DSC thermograms of Compound **XIIA**. It shows a melting transition at 95.0°C on the heating scan. On the cooling scan it reveals an isotropic to nematic phase transition at 94.0°C, a nematic to smectic A phase transition at 89.1°C, and a crystallization temperature at 69.4°C. Figure 2 shows the typical schlieren nematic phase and focal-conic fan smectic A texture exhibited by Compound **XIIA** upon cooling from isotropic phase. Comparing the thermal behavior of this series of compounds with that of corresponding compounds in the previous series demonstrates that incorporation of a naphthyl ring in the mesogenic core enhances the tendency toward the formation of a mesophase. Unfortunately, the melting transitions also increase about 20 to 40°C from their corresponding fluorinated diphenylacetylenic compounds. Compounds **IA–VIA** and **XA–XIIA**, which contain a lateral fluoro-substituent, exhibit relatively lower melting transitions than the corresponding compounds without the lateral fluoro-substituent.

Table 3 reports the thermal transition temperatures and corresponding enthalpy changes of Monomers **IM–XIIM**. No monomers show mesomorphic behav-

TABLE 2. Thermal Transitions and Thermodynamic Parameters of Compounds **IA–XIIA**

Compound	n[a]	R_m[a]	X[a]	Phase transitions, °C (corresponding enthalpy changes, kcal/mol),[b] heating	cooling
IA	3	R_1	H	K 113.8 (7.34) I	I 101.2 (7.38) K
IIA	6	R_1	H	K 96.0 (8.03) I	I 76.4 (7.50) K
IIIA	11	R_1	H	K 103.7 (12.28) I	I 88.5 (12.65) K
IVA	3	R_1	F	K 63.1 (6.28) I	I 25.8 (5.08) K
VA	6	R_1	F	K 51.6 (5.13) I	I 41.8 $(-)^{c}$ N 39.3 (0.78) S_A 23.2 (3.01) K
VIA	11	R_1	F	K 74.8 (10.94) I	I 59.9 (10.63) K
VIIA	3	R_2	H	K 156.7 (9.48) I	I 143.0 (9.50) K
VIIIA	6	R_2	H	K 125.2 (6.35) I	I 116.0 $(-)^{c}$ N 105.7 (6.04) K
IXA	11	R_2	H	K 122.9 (11.32) I	I 109.6 (11.80) K
XA	3	R_2	F	K 103.4 (7.21) I	I 98.3 (0.11) N 75.7 (6.10) K
XIA	6	R_2	F	K 83.6 (4.40) I	I 78.8 (0.15) N 63.0 (3.68) K
XIIA	11	R_2	F	K 95.0 (11.1) I	I 94.0 $(-)^{c}$ N 89.1 (0.84) S_A 69.4 (9.31) K

[a] n, R_m, and X according to Scheme 1.

[b] K = crystalline, S_A = smectic A, N = nematic, and I = isotropic.

[c] Overlapped transition.

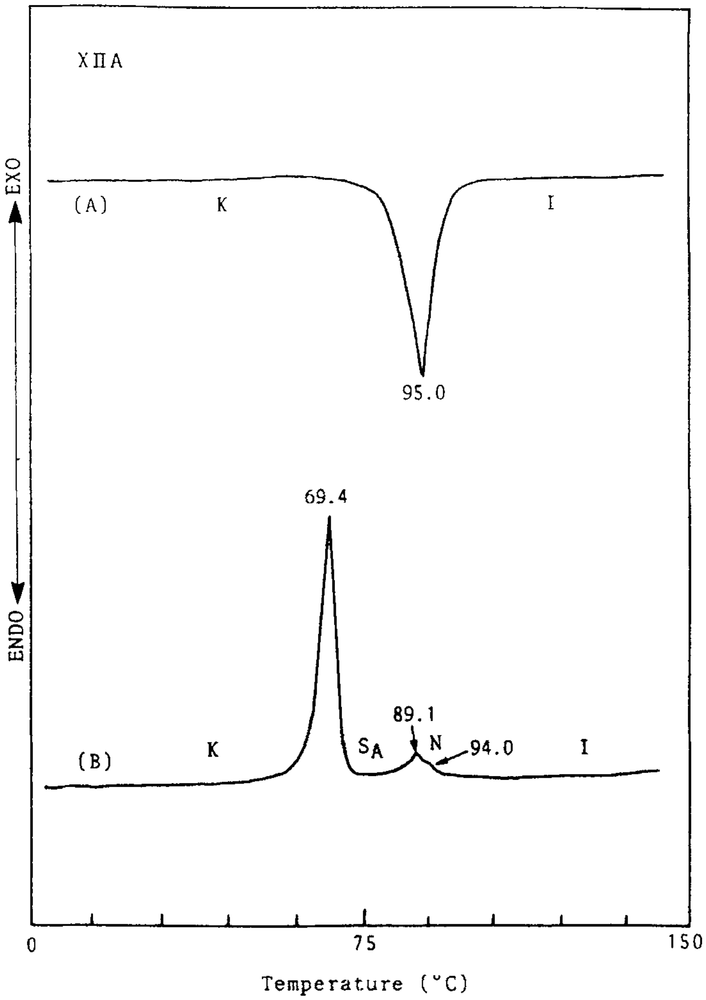

FIG. 1. DSC thermograms (10°C/min) for Compound **XIIA**: (A) heating scan; (B) cooling scan.

ior. This could be due to the bulky methacrylate group. The synthesis of side-chain liquid crystalline polymethacrylates is outlined in Scheme 2. The results of free radical polymerizations of methacrylate monomers by 2,2′-azobisisobutyronitrile (AIBN) as an initiator are summarized in Table 4. All monomers gave reasonable yields in the polymerizations. The molecular weights of these polymers were determined by GPC using a calibration based on polystyrene standards and therefore have only a relative meaning.

Table 4 reports the thermal transitions and thermodynamic parameters of Polymers **IP–XIIP**. Most of these polymers reveal liquid crystalline phases. The phase assignment was conducted by both optical polarizing microscopy and x-ray diffraction measurements. Among Polymers **IP–IIIP** which contain monofluori-

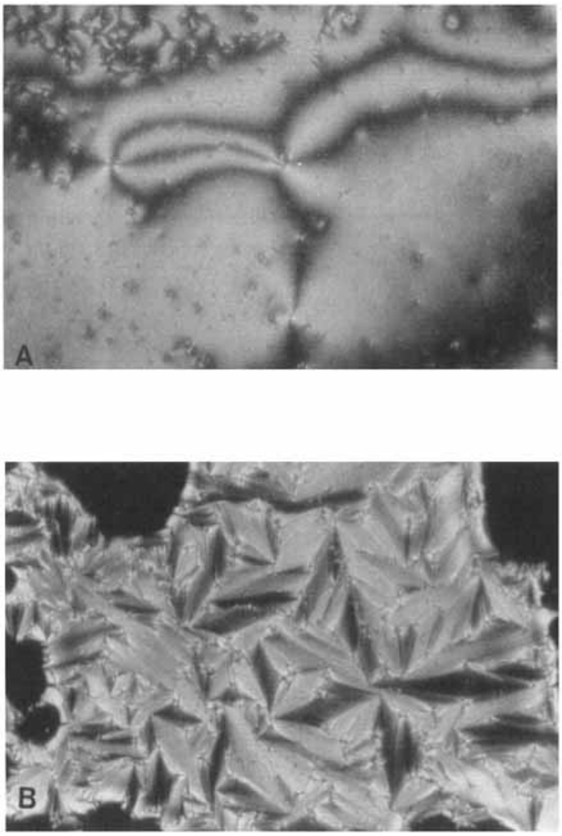

FIG. 2. Optical polarizing micrographs displayed by Compound **XIIA** upon cooling from the isotropic phase: (A) nematic texture obtained at 94°C; (B) S_A texture obtained at 85°C.

nated diphenylacetylenic side groups, Polymer **IP** shows no mesomorphic behavior, Polymer **IIP** reveals an enantiotropic nematic phase, while Polymer **IIIP** exhibits enantiotropic smectic A and smectic B phases. Representative DSC traces for Polymer **IIIP** are presented in Fig. 3. A glass transition at 14.2°C is displayed here, followed by a smectic B to smectic A phase transition at 58.9°C, and a smectic A to isotropic phase transition at 88.5°C on the heating scan (Curve A). The cooling scan (Curve B) looks almost identical to the heating scan, except that a very small supercooling (less than 10°C) is observed for two exothermic transitions. Figure 4 presents the temperature-dependent x-ray diffraction diagrams obtained from powder samples of **IIIP** at 70 and 50°C. A broad reflection at wide angles (associated with the lateral packings) and a sharp reflection at low angles (associated with the smectic layers) are respectively shown by all curves. Curve A presents a diffuse reflection at about 4.56 Å, which corresponds to lateral spacing of two mesogenic side groups, and a sharp first-order reflection at 17.21 Å, which corresponds to smectic layers. This result is also in agreement with the optical microscopic observa-

TABLE 3. Phase Transitions and Phase Transition Enthalpies of Monomers **IM–XIIM**

Monomer	n[a]	R_m[a]	X[a]	Phase transitions, °C (corresponding enthalpy changes, kcal/mol),[b] heating cooling
IM	3	R_1	H	*K* 76.7 (3.06) *I* *I* 35.7 (0.48) *K*
IIM	6	R_1	H	*K* 65.9 (8.76) *I* *I* 34.6 (8.07) *K*
IIIM	11	R_1	H	*K* 83.5 (15.17) *I* *I* 58.6 (14.17) *K*
IVM	3	R_1	F	*K* 79.7 (4.53) *I* *I* 57.4 (2.75) *K*
VM	6	R_1	F	*K* 67.6 (10.14) *I* *I* 25.6 (7.25) *K*
VIM	11	R_1	F	*K* 60.9 (13.97) *I* *I* 42.2 (13.75) *K*
VIIM	3	R_2	H	*K* 117.5 (8.75) *I* *I* 69.0 (7.81) *K*
VIIIM	6	R_2	H	*K* 58.7 (5.92) *I* *I* 11.3 (0.12) *K*
IXM	11	R_2	H	*K* 74.9 (7.74) *I* *I* 56.0 (7.16) *K*
XM	3	R_2	F	*K* 118.8 (11.41) *I* *I* 73.4 (8.45) *K*
XIM	6	R_2	F	*K* 53.7 (6.52) *I* *I* 24.5 (0.41) *K*
XIIM	11	R_2	F	*K* 65.4 (8.76) *I* *I* 49.0 (8.34) *K*

[a] n, R_m, and X according to Scheme 1.

[b] K = crystalline and I = isotropic.

tion which shows a characteristic smectic A texture. When the measuring temperature has been further cooled to 50°C, the *d* spacing of first-order reflection changes to 17.37 Å and the wide-angle reflection becomes very sharp (Curve B). It demonstrates the formation of a smectic B phase. Among Polymers **IVP–VIP** which contain difluorinated diphenylacetylenic side groups, Polymers **IVP** and **VP** reveal no

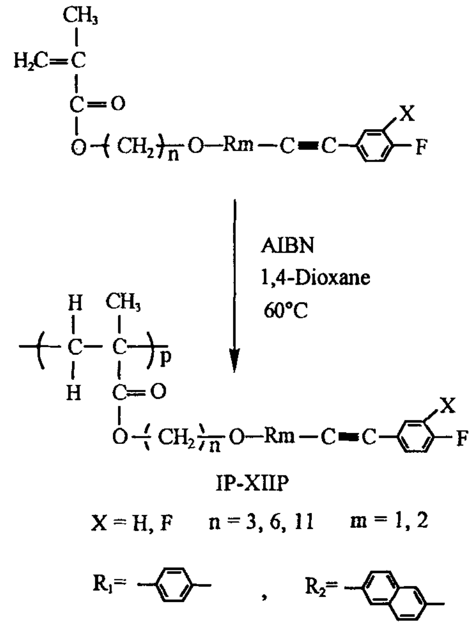

polymer	IP	IIP	IIIP	IVP	VP	VIP	VIIP	VIIIP	IXP	XP	XIP	XIIP
Rm	R_1	R_1	R_1	R_1	R_1	R_1	R_2	R_2	R_2	R_2	R_2	R_2
n	3	6	11	3	6	11	3	6	11	3	6	11
X	H	H	H	F	F	F	H	H	H	F	F	F

SCHEME 2. Synthesis of methacrylate Polymers **IP-XIIP**.

mesomorphic behavior while Polymer **VIP** shows an enantiotropic smectic A phase. Representative DSC traces for Polymer **VIP** are also presented in Fig. 3. Polymer **VIP** shows a glass transition at 2.2°C and a smectic A to isotropic phase transition at 61.9°C on its heating scan (Curve C). The optical polarizing micrograph (Fig. 5) reveals a typical S_A texture for Polymer **VIP**. As can be seen from data reported in Table 4, as the spacer length increases, the glass transition temperature decreases while the tendency toward smectic phase increases. Incorporation of a lateral fluoro-substituent in the mesogenic core decreases the possibility of a mesophase to form.

In the third series of polymers which contain monofluorinated naphthylphenylacetylenic side groups, all three Polymers **VIIP-IXP** show mesomorphic behavior. Polymers **VIIP** and **VIIIP** reveal an enantiotropic nematic phase while Polymer **IXP** exhibits an enantiotropic smectic A phase. Among Polymers **XP-XIIP** which contain difluorinated naphthylphenylacetylene, both Polymers **XP** and **XIP** display no mesomorphic behavior while Polymer **XIIP** presents an enantiotropic smectic A phase. The results, which are also summarized in Table 4, illustrate that incorporation of a naphthyl ring instead of a phenyl ring in the mesogenic core will enhance the formation of a liquid crystallince phase and also increase the thermal stability of

TABLE 4. Phase Transitions and Phase Transition Enthalpies of Polymers **IP-XIIP**

Polymer	n[a]	R_m[a]	X[a]	$\overline{M}_n$	Phase transitions, °C (corresponding enthalpy changes, kcal/mru[b]),[c]	
					heating	cooling
IP	3	R_1	H	12,354	G 53.5 I	I 46.2 G
IIP	6	R_1	H	9,519	G 33.3 N 61.4 (0.25) I	I 56.0 (0.23) N 25.6 G
IIIP	11	R_1	H	7,547	G 14.2 S_B 58.9 (0.46) S_A 88.5 (0.71) I	I 78.1 (0.63) S_A 54.4 (0.36) S_B 14.1 G
IVP	3	R_1	F	10,830	G 36.6 I	I 28.4 G
VP	6	R_1	F	4,771	G 10.0 I	I 4.7 G
VIP	11	R_1	F	15,755	G 2.2 S_A 61.9(0.88) I	I 48.8 (0.84) S_A − 6.6 G
VIIP	3	R_2	H	5,004	G 73.1 N 133.5 (0.05) I	I 128.3 (0.04) N 61.8 G
VIIIP	6	R_2	H	3,830	G 38.7 N 107.8 (0.11) I	I 102.6 (0.09) N 30.7 G
IXP	11	R_2	H	3,771	G 5.8 S_A 64.1 (0.24) I	I 56.4 (0.31) S_A −0.5 G
XP	3	R_2	F	5,833	G 53.5 I	I 49.7 G
XIP	6	R_2	F	2,857	G 17.7 I	I 7.4 G
XIIP	11	R_2	F	7,706	G 11.0 S_A 83.9 (0.30) I	I 76.2 (0.30) S_A 2.7 G

[a] n, R_m, and X according to Scheme 2.

[b] mru = mole repeating unit.

[c] G = glassy, S_A = smectic A, S_B = smectic B, N = nematic, and I = isotropic.

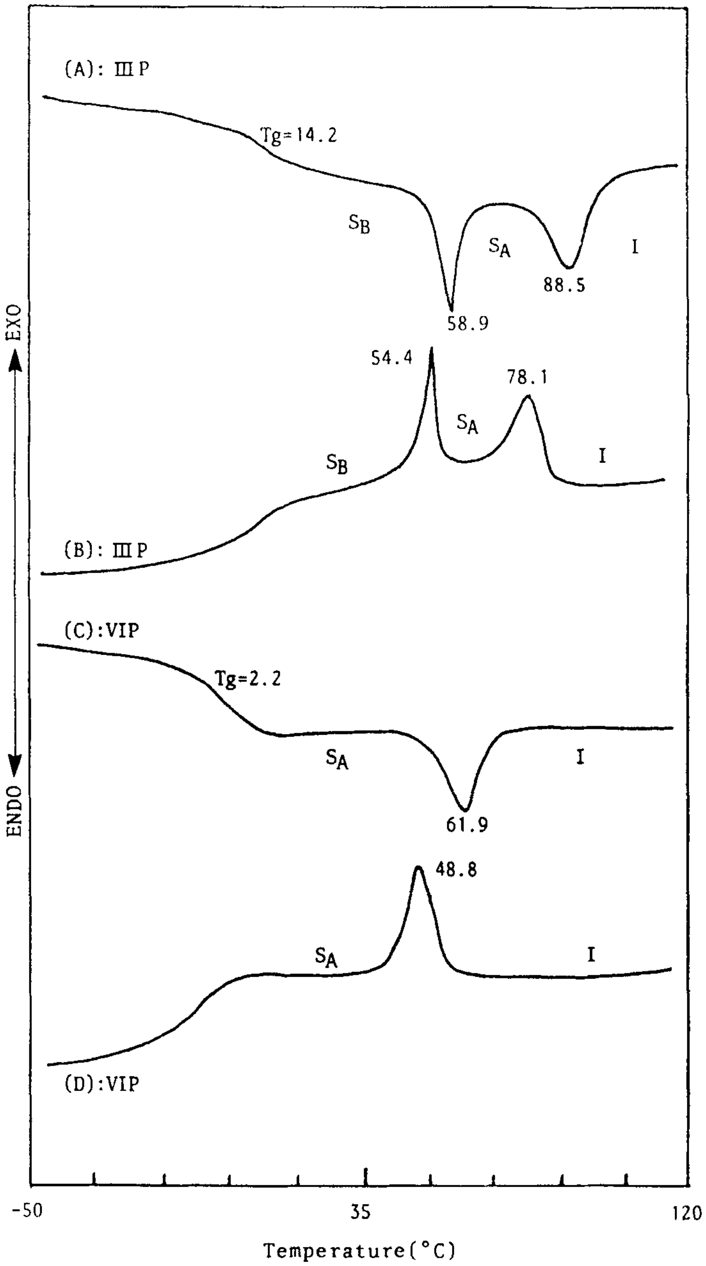

FIG. 3. DSC thermograms (10°C/min) for Polymers **IIIP** and **VIP**: (A) **IIIP**, heating scan; (B) **IIIP**, cooling scan; (C) **VIP**, heating scan; (D) **VIP**, cooling scan.

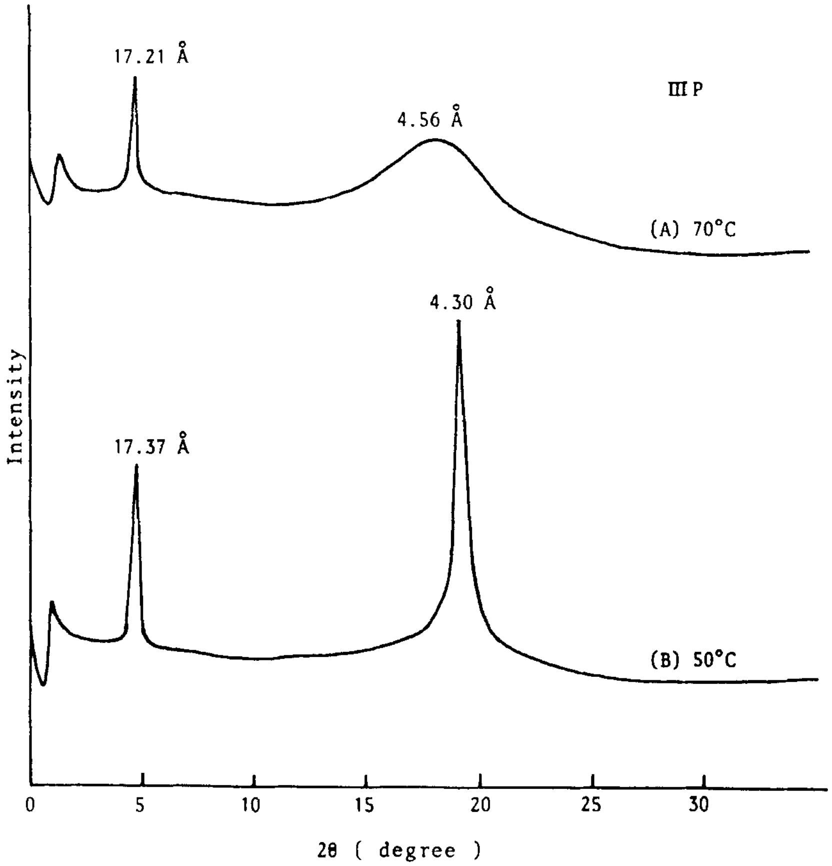

FIG. 4. Temperature-dependent x-ray measurements for Polymer **IIIP** obtained at (A) 70 and (B) 50°C.

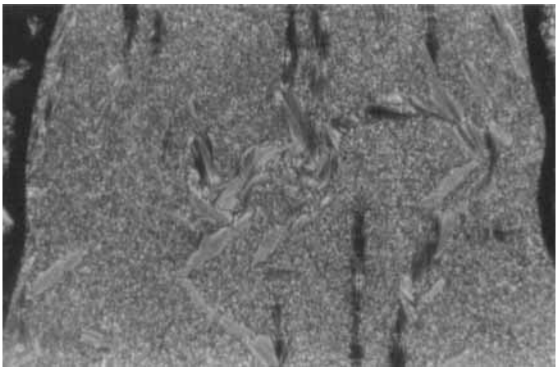

FIG. 5. Optical polarizing micrograph displayed by Polymer **VIP** upon cooling from the isotropic phase: S_A texture obtained at 47°C.

the mesophase. Again, incorporation of a lateral fluoro-substituent into the mesogenic core will decrease the possibility of a mesophase to form.

CONCLUSIONS

Four series of side-chain liquid crystalline polymethacrylates containing fluorinated diphenylacetylenic or naphthylphenylacetylenic side groups were synthesized. The flexible spacer length has a profound influence on the nature and thermal stability of the mesophases formed. Incorporation of a lateral fluoro-substituent into the mesogenic core decreases the possibility of a mesophase to form. However, the replacement of a phenyl ring from the tolane mesogenic core by a naphthyl ring increases dramatically the possibility of a mesophase to form.

ACKNOWLEDGMENT

The authors are grateful to the National Science Council of the Republic of China (NSC84-2815-C009-01-033E) for financial support of this work.

REFERENCES

[1] A. Ciferri, W. R. Krigbaum, and R. B. Meyer, *Polymer Liquid Crystals*, Academic Press, New York, 1982.
[2] L. L. Chapoy, *Recent Advances in Liquid Crystalline Polymers*, Elsevier, London, 1985.
[3] A. Blumstein, *Polymeric Liquid Crystals*, Plenum, New York, 1985.
[4] C. B. McArdle, *Side Chain Liquid Crystal Polymers*, Blackie, Glasgow, 1989.
[5] B. A. Jones, J. S. Bradshaw, M. Nishioka, and M. L. Lee, *J. Org. Chem.*, *49*, 4947 (1984).
[6] M. A. Apfel, H. Finkelmann, G. M. Janini, R. J. Lamb, B. H. Luhmann, A. Price, W. L. Roberts, T. J. Shaw, and C. A. Smith, *Anal. Chem.*, *57*, 651 (1985).
[7] J. S. Bradshaw, C. Schregenberg, H. C. Karen, K. E. Markides, and M. L. Lee, *J. Chromatogr.*, *358*, 95 (1986).
[8] H. J. Coles and R. Simon, *Polymer, 26*, 1801 (1985).
[9] R. F. Coozner and H. Finkelmann, *Makromol. Chem.*, *186*, 2407 (1985).
[10] C. B. McArdle, M. G. Clark, C. M. Haws, M. C. K. Wiltshire, A. Parker, G. Nestor, G. W. Gray, D. Lacey, and K. J. Toyne, *Liq. Cryst.*, *2*, 573 (1987).
[11] C. Pugh and V. Percec, *J. Polym. Sci., Polym. Chem. Ed.*, *28*, 1101 (1990).
[12] C. Pugh and V. Percec, *Mol. Cryst. Liq. Cryst.*, *178*, 193 (1991).
[13] C. Pugh, C. Tarnstrom, and V. Percec, *Ibid.*, *195*, 185 (1991).
[14] C. Pugh and V. Percec, *Chem. Mater.*, *3*, 107 (1991).
[15] C. Pugh, S. K. Andersson, and V. Percec, *Liq. Cryst.*, *10*, 229 (1991).

[16] V. Percec and R. Rodenhouse, *J. Polym. Sci., Polym. Chem. Ed., 29*, 15 (1991).
[17] V. Percec, G. Johansson, and R. Rodenhouse, *Macromolecules, 25*, 2563 (1992).
[18] C. S. Hsu and Y. H. Lu, *Mol. Cryst. Liq. Cryst., 225*, 1 (1993).
[19] Y. H. Lu, K. T. Tsay, C. S. Hsu, and H. L. Chang, *Ibid., 250*, 85 (1994).
[20] C. J. Hsieh, S. H. Wu, G. H. Hsiue, and C. S. Hsu, *J. Polym. Sci., Polym. Chem. Ed., 32*, 1077 (1994).
[21] S. T. Wu, E. Efron, and L. D. Hess, *Appl. Phys. Lett., 44*, 1033 (1984).
[22] K. C. Lim, J. D. Margerum, and A. M. Lackner, *Ibid., 62*, 1065 (1993).
[23] E. J. Corey and P. L. Fuchs, *Tetrahedron Lett., 36*, 3769 (1972).